

Investigation of the characteristics of EUV backward transition radiation generated by 5.7 MeV electrons in mono- and multilayer targets

This content has been downloaded from IOPscience. Please scroll down to see the full text.

2014 J. Phys.: Conf. Ser. 517 012009

(<http://iopscience.iop.org/1742-6596/517/1/012009>)

View [the table of contents for this issue](#), or go to the [journal homepage](#) for more

Download details:

IP Address: 78.140.61.51

This content was downloaded on 10/06/2014 at 03:16

Please note that [terms and conditions apply](#).

Investigation of the characteristics of EUV backward transition radiation generated by 5.7 MeV electrons in mono- and multilayer targets

S R Uglov¹, V V Kaplin¹, A P Potylitsyn¹, L G Sukhikh¹,
A V Vukolov¹ and G Kube²

¹Tomsk Polytechnic University, Lenin avenue, 30, Tomsk, 634050, Russia

²Deutsches Elektronen-Synchrotron (DESY), Notkestrasse 85, 22607, Hamburg, Germany

E-mail: uglov@tpu.ru

Abstract. This paper presents experimental results of a study of radiation in the vacuum ultraviolet and extreme ultraviolet spectral region, generated by electrons with an energy of 5.7 MeV in a multilayer X-ray mirror. The angular distribution of the radiation generated in the rear hemisphere from the input surface of the target was measured. The contribution to the radiation yield caused by the periodic structure of the multilayer target was experimentally investigated.

1. Introduction

Imaging of transverse beam profiles based on backward transition radiation (BTR) in the visible region of the spectrum is widely used in modern linear accelerators. This kind of beam diagnostics is usually termed optical transition radiation (OTR) monitor. However, the latest results from new generation VUV and X-ray free-electron lasers, such as LCLS (USA), FLASH (Germany), and SACLA (Japan), have demonstrated that there are serious limitations in using such a beam diagnostics because of instabilities arising in individual bunches. This microbunching causes the appearance of coherent effects (quadratic dependence of the radiation power on the microbunch population), which makes it impossible to use standard imaging techniques based on OTR. To overcome this problem it is possible to measure at smaller photon wavelengths, and in Ref. [1] it was proposed to use BTR in the spectral region of the extreme vacuum ultraviolet (EUV). In this case, the main problem is connected with the quite small spectral density of the radiation yield from conventional radiators, consisting of a homogeneous substance (monolayer targets). This requirement of a high spectral density is driven by the fact that for beam diagnostics in modern linear accelerators it is necessary to resolve beam profiles on the level of individual bunches, which typically contain $10^9 - 10^{10}$ electrons.

The radiation yield of BTR in the EUV region can be increased by using a large target tilt angle of about 60 – 70 degrees (with the angle defined between the normal of the target surface and the beam axis), but this results in a significant beam image distortion due to the depth of field effect. On the other hand, OTR monitors are usually implemented with smaller target tilt angles of 22.5 or 45 degrees. In order to achieve a comparable tilt angle and sufficient radiation yield in the EUV region, the use of a periodic multilayer structure as radiator is



considered to be more promising in comparison to a conventional monolayer target. Such a periodic multilayer structure is known as a multilayer X-ray mirror. Considering the mechanism of BTR generation as reflection of the relativistic electron field (so called pseudo-photons) at the target structure, it is to expect that the use of a multilayer interference structure with an appropriate period will result in an increase of the target reflectivity and the radiation yield, respectively. The energy of the additional radiation photons will be distributed in a narrow spectral range which is determined by the Bragg diffraction from a periodic structure. Indeed, if the mirror is placed under Bragg condition, X-rays can be scattered out and two processes, diffracted transition radiation (DTR) and parametric X-ray radiation (PXR) can occur. There are several theoretical and experimental investigations [2, 3, 4, 5, 6, 7] connected with these types of radiation. The mechanism of radiation generation in multilayer X-ray mirrors (MXM) are similar to the mechanisms of PXR and DTR generation from periodic crystal structures. Experimental studies [4, 5, 6, 7] have been carried out for MXM generated in the X-ray region with photon energies of $E_\gamma = 6 - 15$ keV. Recently, experimental investigations of the MXM mechanism in the EUV region started at Tomsk Polytechnic University using a 5.7 MeV electron beam [8, 9]. This paper presents the results of a measurement of the angular distributions of EUV radiation from a multilayer radiator consisting of 50 Mo/Si bilayers placed onto a silicon substrate. The results are compared with the ones obtained from a monolayer radiator consisting of a silicon wafer coated with a layer of molybdenum.

2. Experimental setup

The experiment was carried out at the external electron beam of the the microtron M-5 of Tomsk Polytechnic University with a total electron energy of $E_e = 5.7$ MeV. The pulse repetition frequency amounted to 25 Hz, and the pulse duration of the extracted beam was $0.4 \mu\text{s}$. The scheme of the accelerator complex together with the experimental setup are shown in figures 1 and 2. The studies were carried out at the experimental chamber (16) of beam line II, cf. figure 1. The electron beam extracted from the microtron passed a bending magnet (3), a collimator system (4,6,7), and a second bending magnet (9). Using the second bending magnet it was possible to reduce the background generated by bremsstrahlung in the collimators. The transverse beam shape at the target (14) in the center of the the experimental chamber was close to a circle with a diameter of 2 – 3 mm, and the beam charge amounted to $q \approx 4$ pC per pulse of beam ejection. The monitoring of the beam current of accelerated electrons was carried out by a NaI (Tl) detector (17) located at a distance of 1200 mm behind the target.

The radiation yield in the EUV range was measured by the secondary electron multiplier SEM-6 (13). The detector was located in the median plane of the accelerator at a distance of 140 mm from the target onto a rotator that allowed to scan the angular distribution of the radiation emitted from the target in the range of $\theta_D = 20^\circ$ up to $\theta_D = 160^\circ$ with respect to

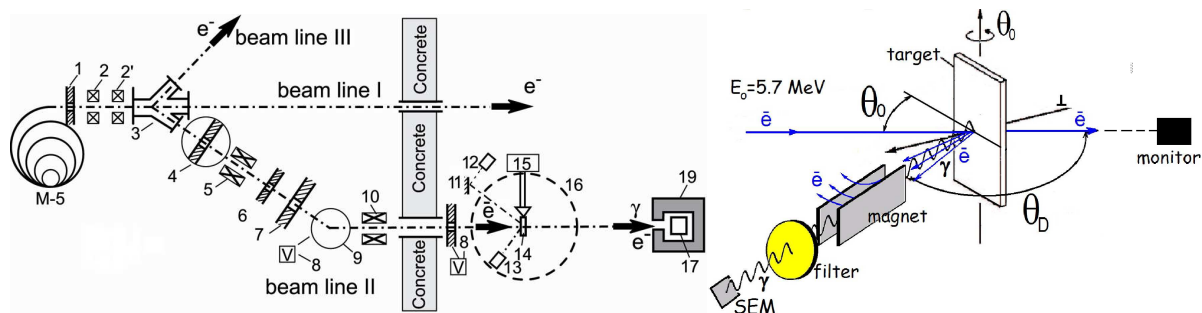


Figure 1. Scheme of the accelerator complex.

Figure 2. Experimental scheme.

the electron beam axis. Permanent magnets and diaphragms were mounted between target and detector along the direction of radiation propagation for cleaning the photon beam from electrons scattered at the target. To eliminate the influence of stray magnetic fields on the electron beam, rare-earth permanent magnets were placed inside an iron box with two reach-through holes. The detection and data acquisition system for the EUV radiation consisted of the SEM-6 secondary electron multiplier, a preamplifier U3-33, an amplifier BUS2-97, a CAMAC shaper and a counter. The SEM-6 was operated in counting mode. To prevent pile-up effects, the detector load was controlled every 100 pulses of the accelerator and, as a rule, did not exceed 50 counts per 100 pulses. The spectral range of the registered radiation was defined by the spectral sensitivity of the SEM-6 [10] and the absorption filter set directly in front of the entrance window of the detector. The entrance window of the SEM-6 had a diameter of $D_0 = 10$ mm. In the experiment however, the size of this window was limited by diaphragms, either with a diameter of $D_1 = 8$ mm in the measurements with filter, or with a diameter of $D_2 = 2.5$ mm in the measurement without. The detector was surrounded by a lead shielding with 10 mm thickness.

As periodic target, a multilayer X-ray mirror consisting of 50 Mo/Si bilayers with a period of $d = 113.2 \text{ \AA}$ was used. The multilayer was sitting onto a silicon wafer with dimensions of $40 \times 40 \times 0.53 \text{ mm}^3$. The thicknesses of the alternating Si and Mo layers were $a = 79.2 \text{ \AA}$ and $b = 34 \text{ \AA}$ ($a + b = d$), respectively. The substrate was a Si (100) wafer of p-type (boron doping), the cut plane was tilted by $1.5 - 2$ degrees with respect to the (100) plane. Figure 3 shows the spectral reflectivity curve for a photon incidence angle of 22.5° .

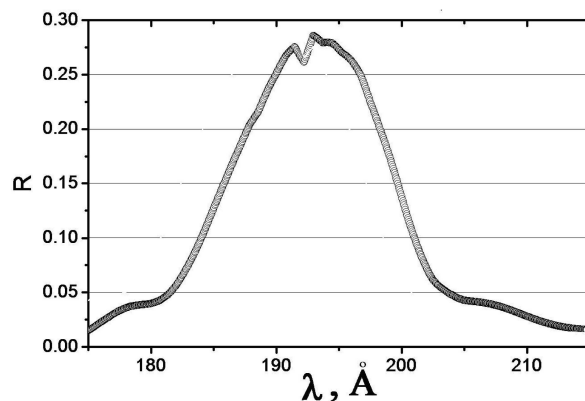


Figure 3. Spectral reflectivity curve of the Mo/Si mirror at an angle of incidence of 22.5° .

The second target consisted of a silicon wafer with dimensions of $40 \times 10 \times 0.68 \text{ mm}^3$ and a 50 nm thick Mo layer at the entrance surface. The parameters of this target correspond to the ones from the target described in Ref. [11]. Both targets were mounted onto a motorized goniometer located in the center of the experimental chamber. The target was preliminarily aligned with respect to the electron beam axis by means of a laser level. In the experiment, the electron beam was steered onto the target with the corrector (10) and observed with a camcorder (12) and two phosphor screens located below and at the side of the target. The angular distributions were scanned in the plane formed by electron beam axis and target surface normal.

3. Experimental results

For a preliminary test of the experimental setup, angular distributions of BTR generated from a polished Si wafer with $250 \mu\text{m}$ thickness and a polished Al foil with $1 \mu\text{m}$ thickness were measured. The results are shown in figures 4 and 5. The solid lines indicate the results of a theoretical calculation of the BTR angular distribution according to the theory [12]. Both calculations

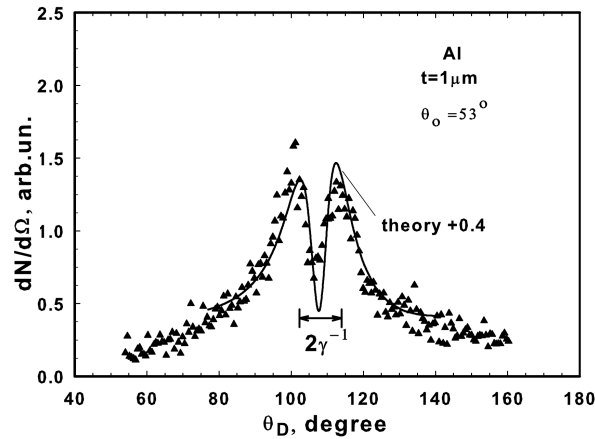


Figure 4. Experimental (triangles) and theoretical (solid curve shifted upwards on 0.4) angular distributions of BTR for the 1 μm thick Al foil and $\theta_0 = 53^\circ$.

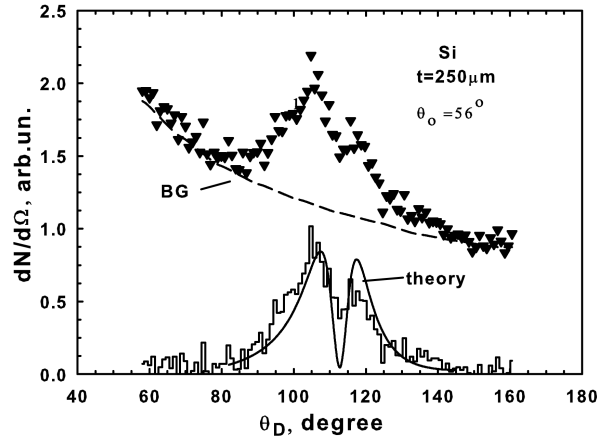


Figure 5. Experimental and theoretical angular distributions of BTR for the 250 μm thick Si wafer and $\theta_0 = 56^\circ$; triangles – experimental data, dashed curve – background, histogram – experimental data without background, solid curve – theoretical distribution.

show a good agreement compared to the experimental data, the expected angular distance $\Delta\theta_D = 2\gamma^{-1}$ between the two lobes of the angular distribution is clearly visible. From the figures it can be seen that the angular distribution for the thick Si target has a considerable background contribution (BG) in comparison to the thin Al target. The nature of this background radiation is bremsstrahlung and characteristic radiation generated by electrons into the bulk of the target.

The main goal of the experiment was to demonstrate that the radiation yield in the EUV region emitted from the multilayer target is larger than the one from the monolayer target because of the additional MXM contribution. According to [2, 3, 4], the expected MXM excess should be observed at the photon energy E_γ defined by:

$$E_\gamma = \hbar\omega = \frac{2\pi\hbar c}{d} \frac{\sin\theta_0}{\beta^{-1} - \sqrt{\varepsilon(\omega)} \cos\theta_D}, \quad (1)$$

with $\beta = v/c$ the reduced electron velocity, d the multilayer structure period, $\varepsilon(\omega) = 1 - [a(1 - \varepsilon(\omega)_{Mo}) + b(1 - \varepsilon(\omega)_{Si})] / d$ the dielectric constant averaged over a structure period, and $\varepsilon(\omega)_{Mo}$, $\varepsilon(\omega)_{Si}$ the dielectric constants of pure molybdenum and silicon. θ_0 is the Bragg angle and θ_D the angle of observation.

According to equation (1), the detection of the radiation component arising from the periodic mirror structure would in principle be possible by exploiting the radiation spectrum using a detector with sufficient energy resolution. However, the photon counting scheme applied in this experiment gave no access to the radiation spectrum. Therefore, the detection of the radiation component of interest was done based on the analysis of angular distributions. Unfortunately, the MXM component is emitted in the same direction as ordinary BTR.

Measurements of angular distributions were carried out for a Bragg angle $\theta_0 = 67.5^\circ$ by scanning the detector angle θ_D around the angle $2\theta_0 = 135^\circ$. For these parameters and assuming $d = 113.2 \text{ \AA}$ and $\theta_D = 135^\circ$, radiation with a photon energy of $E_\gamma = 60 \text{ eV}$ should be generated according to equation (1).

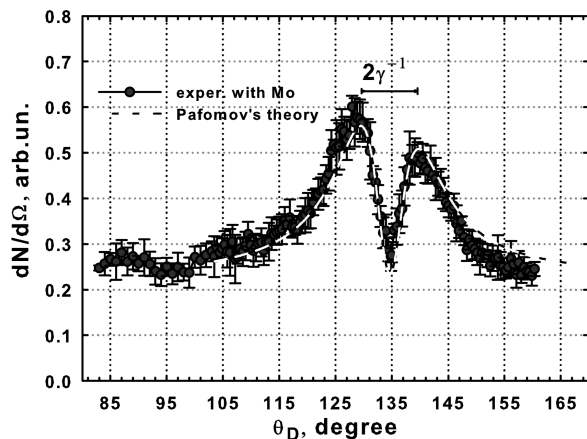


Figure 6. Experimental and theoretical angular distributions of radiation for the Si wafer coated with molybdenum and $\theta_0 = 67.5^\circ$; points – experimental data, dashed curve shifted upwards on 0.25 – theoretical distribution calculated according to [12].

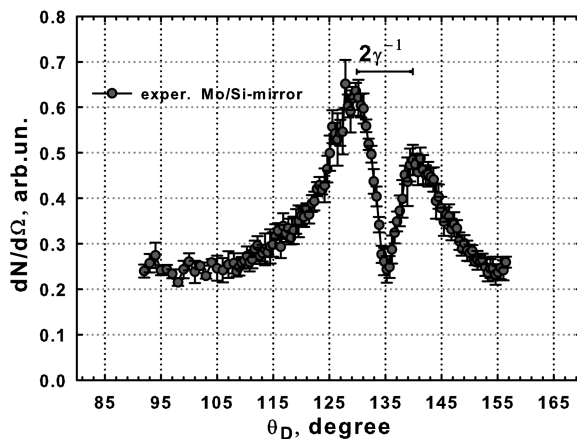


Figure 7. Experimental angular distribution of radiation from the multilayer Mo/Si structure and the Bragg angle $\theta_0 = 67.5^\circ$.

Figures 6 and 7 show measured angular distributions for the multilayer Mo/Si target and the Mo-coated silicon wafer target. For these measurements, the diameter of the diaphragm placed in front of the SEM-6 detector amounted to $D_2 = 2.5$ mm. In this case, the detection efficiency for EUV radiation was solely determined by the detection efficiency of the SEM-6 [10].

Comparing the measured angular distributions in figures 6 and 7, the intensities and the distribution shapes do not show a significant difference because of the rather intense component of conventional BTR in the EUV region which is generated at the entrance surfaces of both targets. Unfortunately, the comparison of these curves gives no direct hint for the observation of an additional MXM contribution. It is necessary to note that the relative intensity values plotted in both figures were obtained by normalizing the SEM-6 count rate with the beam current monitor readings from the NaI (Tl) detector located behind the target, cf. figure 1. As consequence, the quite different target thicknesses have to be considered.

In order to overcome the thickness dependence, in the subsequent measurements both targets were mounted together onto the goniometer close to each other. The radiation under investigation was generated at the first target, the second one was used to compensate the total thickness, and both targets could easily interchange their places.

For a discussion of an additional reduction of the EUV BTR intensity, figure 8 shows BTR spectra for Mo (curve 1), Si (curve 2) and SiO_2 (curve 3), calculated in the range from 6 eV up to 100 eV. They were computed at the maximum of the horizontal profile of the angular distribution. Note that the shape of the spectral distribution of BTR is almost independent on the direction of the radiation inside the cone. Curves 4 and 5 show the transmission coefficients of the Al filter with a thickness of $1 \mu\text{m}$. Curve 5 demonstrates the additional influence of two oxide layers (Al_2O_3) of equal thickness at both sides of the filter surface, assuming an overall layer thickness of $2t_{\text{Al}_2\text{O}_3} = 40$ nm. The calculations were based on the database “EPDL-97” [13] for optical constants.

As can be seen from figure 8, the main yield of BTR (curves – 1,2,3) is expected to be in the range of photon energies $E_\gamma < 40$ eV, whereas the energy of the MXM photons generated by the periodic target structure is in the range of 54 – 70 eV. Therefore, by using an Al filter

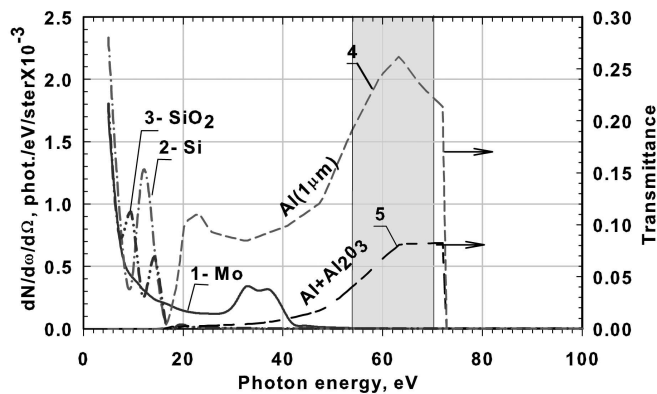


Figure 8. Spectral angular density of BTR at the maximum of the angular distribution for three materials. Mo: curve 1, Si: curve 2, and SiO₂: curve 3. Curves 4 and 5 show the photon transmittance through a 1 μm thick Al foil without and with additional Al₂O₃ layers ($2t_{Al_2O_3} = 40$ nm). The gray region indicates the expected MXM region.

(curve 5) it is possible to suppress sufficiently the main component of the EUV BTR without significant suppression of the radiation in the energy range of MXM photons.

Figures 9 and 10 show the measurements of the angular distributions using a 1 μm thick Al filter. In these measurements, the diaphragm diameter in front of the SEM-6 was increased up to $D_1 = 8$ mm. Figure 9 (data set 1) shows the angular distribution for the radiation from a silicon target with molybdenum coating. Data sets 2 and 3 correspond to angular distributions measured with homogeneous Si targets. Data set 2 is measured for a target with a polished surface, data set 3 was measured for a target with a rough surface (the reverse side of the multilayer mirror substrate). As can be seen from this figure, no distinctive features of BTR can be observed, indicating that the photons of BTR were absorbed by the Al filter. At the same time, in the angular distribution of radiation from a multilayer target (data set 1) it is possible to observe a double-humped structure with a downward excursion at $\theta_D = 135^\circ$ and a characteristic distance between the peaks of $\Delta\theta_D \simeq 10^\circ$, see figure 10. For a better comparison, data set 1 from figure 9 is plotted additionally and named data set 2 in figure 10.

Thus, according to the results of the angular distribution measurements, an additional component of radiation is present in the radiation generated at a multilayer target. The origin of this component can be explained by the generation mechanisms of PXR and/or DTR in a

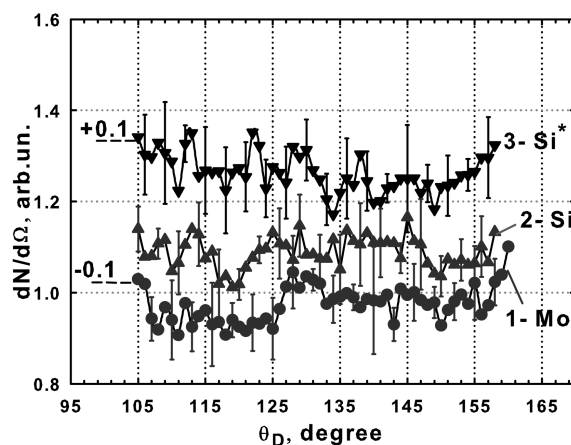


Figure 9. Angular distribution of radiation from uniform targets using the 1 μm thick Al filter. 1: Mo target, 2: polished Si plate, 3: unpolished Si plate.

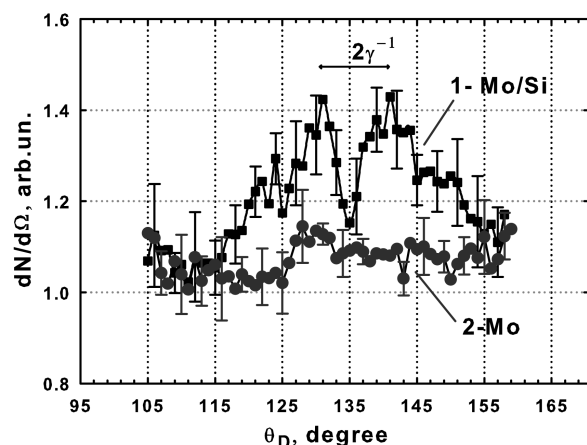


Figure 10. The angular distribution of radiation using the 1 μm thick Al filter. 1: radiation from multilayer Mo/Si mirror, 2: radiation from uniform Mo target.

periodic structure of a multilayer X-ray mirror. Taking into account the data concerning the detector efficiency from [10] together with the calculated transmittance of the 1 μm thick Al foil, a rough estimate of $dN/d\Omega \approx 5.6 \times 10^{-4}$ ph/ \bar{e} /sr for the angular density of MXM at the peak position can be stated.

4. Conclusion

The experimental investigation of EUV BTR angular distributions generated by 5.7 MeV electrons in multilayer structures and targets with homogeneous composition indicates that the periodic structure of the target makes an additional contribution to the radiation intensity. The observed angular distribution of the additional contribution in the form of a double-humped distribution with a minimum at $\theta_D = 135^\circ$ and peaks at $\theta_D = 130^\circ$ and $\theta_D = 140^\circ$ can be explained by the mechanisms of PXR and/or DTR generation from the periodic structure of a multilayer X-ray mirror [2, 3, 4, 5, 6]

From the experimental data, it can be seen that there is a significant background contribution from characteristic radiation and bremsstrahlung of the target material. This background can be reduced to a large extent by reducing the thickness of the multilayer structure substrate down to several microns. Measurements carried out with a thin Al target (figure 4) illustrate the possibility of obtaining angular distributions with a high signal-to-noise ratio.

The estimation of an absolute yield of the detected MXM is difficult because of two reasons: the EUV photon efficiency of the SEM-6 detector is not precisely known, and experimental data concerning the transmittance of the Al filter used in the experiment are missing, especially taking into account the contribution of an additional Al_2O_3 oxide layer. However, as rough estimate a value of $dN/d\Omega \approx 5.6 \times 10^{-4}$ ph/ \bar{e} /sr for the angular density of MXM at the peak position can be stated. This result is close to the value $dN/d\Omega \approx 4.6 \times 10^{-4}$ ph/ \bar{e} /sr calculated according to the Nasonov's theory [5].

Acknowledgments

We would like to thank I.A. Artyukov for his help with the manufacturing of the Mo/Si targets. This work was partially supported by the Russian Ministry of Education and Science program "Nauka", Grant 2456, and by the Russian Foundation for Basic Research, Grant 14-02-01032.

References

- [1] Sukhikh L G, Bajt S, Kube G, Popov Yu A, Potylitsyn A P and Lauth W 2012 *Proc. International Particle Accelerator Conference IPAC'12 (New Orleans, Louisiana, USA)*, p 819, MOPPR019
- [2] Andre J-M, Barchewitz R, Bonnelle C and Pardo B 1993 *J. Opt. Paris* **24** 31.
- [3] Andre J-M, Pardo B and Bonnelle C 1999 *Phys. Rev. E* **99** 968
- [4] Kaplin V V, Uglov S R, Zabaev V N, Piestrup M A, Gary C K, Nasonov N N and Fuller M K 2000 *Appl. Phys. Lett.* **76** 3647
- [5] Nasonov N N, Kaplin V V, Uglov S, Piestrup M and Gary C 2003 *Phys. Rev. E* **68** 036504
- [6] Nasonov N N, Kaplin V V, Uglov S R, Zabaev V N, Piestrup M and Gary C 2005 *Nucl. Instrum. and Meth. B* **227** 41
- [7] Kaplin V V, Uglov S R, Sohoreva V V, Bulaev O F, Voronin A A, Piestrup M, Gary C and Fuller M 2009 *Nucl. Instrum. and Meth.* **267** 777
- [8] Uglov S R, Zabaev V N, Kaplin V V and Kuznetsov S I 2012 *Jour. of Phys.: Conf. Ser.* bf 357 012012
- [9] Uglov S R, Zabaev V N and Kaplin V V 2013 *Nucl. Instrum. and Meth. B* **309** 79
- [10] Einbund M R and Polenov B V 1981 *Secondary electron multipliers and their application* (Moscow: Energoatomizdat) (in Russian)
- [11] Sukhikh L G, Krambrich D, Kube G, Lauth W, Popov Yu A and Potylitsyn A P 2011 *Proc. 10th European Workshop on Beam Diagnostics and Instrumentation for Particle Accelerators DIPAC'11 (Hamburg, Germany)* p 544, WEOA02
- [12] Pafomov V E, 1971 *Proceedings P.N. Lebedev Physics Institute, ed. by D.V. Skolbel'tsyn* **44** (New York: Consultants Bureau) 25-157
- [13] www.esrf.fr/computing/expg/subgroups/theory/DABAX/dabax.html